

Batch and Fixed Bed Adsorption of Pb(II) from Aqueous Solution using EDTA Modified Activated Carbon Derived from Palm Kernel Shell

Aloysius Akaangee Pam,^{a,b} Abdul Halim Abdullah,^{a,c,*} Tan Yen Ping,^a and Zulkarnain Zainal^a

Activated carbons were synthesized by thermochemical treatment of palm kernel shells (AC-PKS) and modified with ethylenediaminetetraacetic acid (AC-EDTA). The developed products were characterized by the surface area, porosity, and pH of point zero charge and were used for removal of Pb(II) ions from aqueous solution. The AC-PKS exhibited higher BET surface area (1559.9 m²/g) than the AC-EDTA (1100.7 m²/g). The influence of solution pH, adsorbent dose, initial Pb(II) ion concentration, and temperature on the removal of Pb(II) ions were examined and optimized. The adsorption of Pb(II) on AC-PKS and AC-EDTA fitted the pseudo-second-order kinetics model and the Langmuir model isotherm, respectively. The optimum conditions for sorption of Pb(II) were at the initial Pb(II) concentration of 150 mg/L, dosage 0.35 g (AC-PKS) and 0.25 g (AC-EDTA), and pH 4. Thermodynamic studies showed that the adsorption process was spontaneous and endothermic. The AC-PKS and AC-EDTA both demonstrated high Q_{\max} of 80.6 mg/g and 104 mg/g, respectively, for Pb(II) adsorption. The adsorption data also fitted the Thomas fixed-bed adsorption model.

Keywords: Activated carbon; Activation; Palm kernel shell; Characterization; Breakthrough time

Contact information: a: Chemistry Department, Faculty of Science, Universiti Putra Malaysia, 43400 UPM Serdang, Selangor Darul Ehsan, Malaysia; b: Chemistry Department, Faculty of Science, Federal University Lokoja, P.M.B. 1154, Lokoja, Nigeria; c: Material Synthesis and Characterization Laboratory, Institute of Advanced Technology, Universiti Putra Malaysia, 43400 UPM Serdang, Selangor Darul Ehsan, Malaysia; *Corresponding author: halim@upm.edu.my

INTRODUCTION

Pollution of water bodies by heavy metals due to manufacturing and mining industries is a well-documented international concern. The presence of these metals in industrial wastewater constitutes serious environmental problems due to their non-biodegradable properties and toxicity (Kampalanonwat and Supaphol 2014). Some of the metals hazardous to humans include lead, cadmium, mercury, arsenic, copper, zinc, and chromium (Sulaymon *et al.* 2013). Pb(II) is toxic and poses harmful effects towards living organisms even at low concentrations. Major sources of lead include mining wastes, chemical industries, lead acid storage batteries, and ceramic and glass industries (Biswas and Mishra 2015). Therefore, it is imperative to remove Pb(II) from wastewater before discharging it into water bodies.

Conventional methods such as ion exchange, membrane filtration, chemical precipitation, solvent extraction, and electrochemical treatment (Mohammadnezhad *et al.* 2017) are available for eliminating heavy metals from industrial wastewater. However,

these techniques have inherent limitations and collateral effects, such as high cost of operation, secondary pollution due to the addition of chemicals in the treatment, and low efficiency (Ding *et al.* 2016). Therefore, the search for efficient and cost-effective remedies is necessary. Adsorption onto suspended particles (solid/liquid interface) is one strategy to eliminate these metallic species. Adsorbents have attracted wide attention in recent years because of the universality of materials and the high efficiency of adsorption (Ding *et al.* 2016), high sorption capacity, cost-effectiveness ratio, and renewability (Tofan *et al.* 2011). Several researchers have examined the feasibility of cheaper substitutes for the preparation of activated carbon in order to eliminate heavy metals from industrial wastewaters either by physical or chemical means, using a variety of starting material such as *Jatropha curcas* fruit shell (Tongpoothorn *et al.* 2011), pine cones (Nowicki *et al.* 2013), and *Citrullus lanatus* rind (Reddy *et al.* 2014).

Malaysia is a leading palm oil producer in the world, and large quantities of palm kernel shells (PKS) are generated as agro-industrial waste. Approximately 4.3 million tons of PKS were generated in 2002 alone, and this creates a huge disposal problem (Jumasiah *et al.* 2005). This study investigated the conversion of PKS to activated carbon (AC) and the modification of the resulting AC with EDTA. EDTA, an aminopolycarboxylic acid, is used mainly as chelating agent due to its strong metal complexing property. The performance of the prepared and modified activated carbon in removing Pb(II) in aqueous solution was evaluated in batch and column studies. The choice of PKS was motivated by its large availability, which makes the material more cost effective. The conversion of these agro products to adsorbents is a possible outlet for economical solid waste-management and could equally offer a solution to water pollution problems.

EXPERIMENTAL

Preparation of Activated Carbons

The palm kernel shell activated carbon (AC-PKS) was prepared by chemical activation with concentrated orthophosphoric acid (H_3PO_4 , 85%; Merck, Darmstadt, Germany). Palm kernel shells (PKS), obtained from the Malaysian Palm Oil Board, were washed with distilled water, dried under the sun, and crushed using a grinder. The PKS powder and H_3PO_4 were mixed at an acid to PKS ratio of 2:1 wt./wt., stirred manually and intermittently for 30 min, and oven-dried at 110 °C for 24 h. The sample was carbonized in a vertical tubular furnace at 600 °C at a heating rate of 10 °C/min for 1 h under nitrogen flow of 20 mL/min. The resulting activated carbon (AC-PKS) was washed several times with warm deionized water until the pH of the wash water was constant, filtered, and oven-dried at 110 °C for 24 h.

The AC-PKS was modified using Na_2EDTA ; 5 g of AC-PKS was refluxed with 100 mL of 0.1 M EDTA solution at 60 °C for 2 h. The modified activated carbon was filtered, washed with warm distilled water under sonication for 10 min to remove any excess EDTA, and finally dried at 100 °C for 24 h. The modified adsorbent is denoted as AC- EDTA.

Characterization of Adsorbents

The specific surface area and porosity of the ACs were determined from nitrogen adsorption desorption isotherm (Quantachrome Autosorb-1, Boynton Beach, FL, USA) using the Brunauer-Emmet-Teller (BET) and Barrett-Joyner-Halenda (BJH) methods, respectively. The pH of the point of zero charge (pHpzc) of the ACs was measured using the pH drift method (Wang *et al.* 2008; Wang and Li 2013).

Batch Adsorption Studies

The stock solution for Pb(II) (1000 mg/L) was prepared by dissolving 1.598 g of lead nitrate (Fisher Scientific, Pittsburgh, PA, USA) into 1000 mL of ultrapure water. The working solution was prepared by diluting the stock solution to desired concentrations.

Batch adsorption experiments were performed to assess the metal removal proficiency of the prepared adsorbents. In a typical experiment, a known mass of the adsorbent was introduced into a series of Erlenmeyer flasks containing 250 mL of 100 mg/L Pb(II) solution. The flasks were shaken at 160 rpm at room temperature for 2 h. At specific time intervals, an aliquot of sample was withdrawn and the concentration of the Pb(II) ions was determined using atomic adsorption spectrophotometer (Thermo Scientific-S series, Waltham, MA, USA). Percentage removal (%) and amount of Pb(II) ions adsorbed (q_t) were computed as follows,

$$q_t = \frac{(C_0 - C_e)V}{M} \quad (1)$$

$$\text{Removal}(\%) = \frac{(C_0 - C_e)}{C_0} \times 100 \quad (2)$$

where C_0 and C_e represent the initial and equilibrium concentrations (mg/L), V is the volume of solution used, and M is the weight of adsorbent (g).

The adsorption of Pb(II) onto AC-PKS and AC-EDTA as a function of contact time, adsorbent dosage, initial Pb(II) concentration, initial solution pH and temperature were investigated. The effect of sorbent dose on the equilibrium uptake of Pb(II) was investigated with adsorbent masses of 0.1 to 0.95 g. Effect of initial concentration was studied using individual metal solution of 50 to 150 mg/L Pb. Metal solutions were adjusted to different pH values (1 to 5) with either 0.1 M NaOH or 0.1 M HCl using a pH meter. The effect of temperature on the adsorption capacity of the adsorbents was investigated in a range of 25 °C to 60 °C in a temperature controlled water bath under optimal conditions. All adsorption experiments were performed in triplicate.

Fixed-Bed Adsorption Studies

Glass columns of 2 cm internal diameter were used in fixed bed experiments. AC-EDTA was packed with different bed heights (2.5 and 4.3 cm) in the column with a layer of glass wool and acid wash sand at the bottom. The Pb(II) solution with initial concentration of 150 mg/L was pumped through the packed column in a down-flow mode with the aid of a peristaltic pump at two different flow rates of 10 and 15 mL/min. The effluent samples were collected at regular intervals and analyzed. The column studies were terminated when the column reached exhaustion.

RESULTS AND DISCUSSION

Physicochemical Characterization of AC-PKS and AC-EDTA

The shape of the adsorption isotherm of AC-PKS and AC-EDTA is depicted in Fig. 1 (a). For AC-PKS, a Type IV (a) isotherm and a slight hysteresis loop of type H4 according to IUPAC 2015 classification isotherm (Thommes *et al.* 2015) was noticeable.

The H4 hysteresis loop is associated with micro-mesoporous materials and the pronounced uptake at the low P/P_0 probably arises from the micropore filling. After modification, a Type I (a) isotherm was observed for AC-EDTA with a decreased adsorption of N_2 at high pressure. This isotherm is related to microporous solids with comparatively small external surfaces. The steep uptake at very low P/P_0 is due to enhanced adsorbate/adsorbent interaction in the narrow micropores (Thommes *et al.* 2015), which could be attributed to additional oxygen group introduced on the surface of the adsorbent from the EDTA.

The pore size distributions of AC-PKS and AC-EDTA shown in Fig. 1(b) revealed that the adsorbents were microporous, with average micropore size in the range of 1.53 to 1.71 nm. The BET surface areas and pore structures for AC-PKS and AC-EDTA are presented in Table 1. The BET surface areas and the pore volumes of AC-EDTA was considerably lower than that of AC-PKS, which could be due to the blockage of internal porosity induced by the formation of new functional groups at the mouth of the pores upon EDTA modification.

The point of zero-charge of the activated carbons, as presented in Fig. 2, was estimated to be 3.5 to 4.0. This result indicated that the surface of the adsorbents was acidic, and the introduction of EDTA did not significantly change the surface properties AC-PKS. It is expected that the adsorbent surface would be positively charged at pH below 3.9 and negatively charged at pH above 3.9.

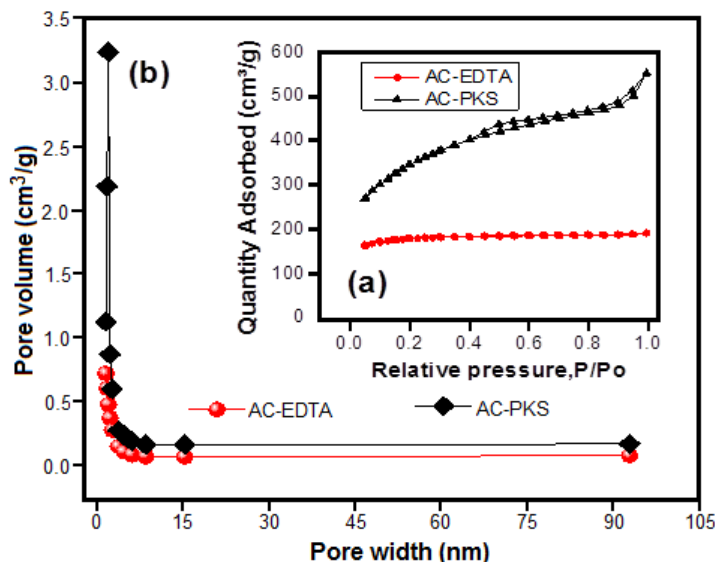
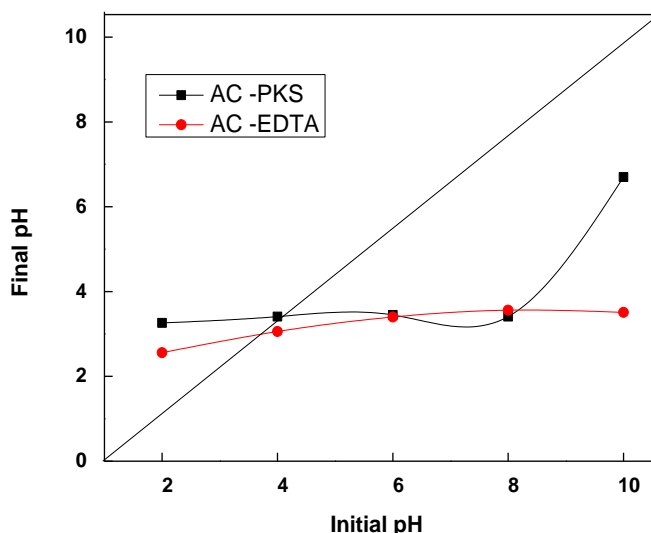


Fig. 1. (a) N_2 adsorption isotherm and (b) pore size distribution for AC-PKS and AC-EDTA

Table 1. Surface Area and Porosity of Activated Carbon

Sample	S_{BET} (m^2/g)	Micropore Size (V_{mic} , cm^3/g)	Micropore Surface Area (S_{mic} , m^2/g)
AC-PKS	1559.9	1.71	139.74
AC-EDTA	1100.7	1.53	172.04

**Fig. 2.** The pH pzc of activated carbons determined by the pH drift method

Batch Adsorption Studies

Effect of adsorbent dosage

The capacity of any sorbent for a given initial concentration of an inorganic pollutant is governed by the adsorbent dosage, making it a vital parameter in the adsorption process. The removal efficiency of Pb(II) by AC-PKS and AC-EDTA (Fig. 3) increased with increasing adsorbent dosage and was attributed to the increase in the availability of sorption sites. However, the amount of Pb(II) adsorbed per unit mass of adsorbent at equilibrium (q_e , mg/g) decreased with the same adsorbent dosage increment. This result was attributed to unsaturation of adsorption sites due to the decrease in the ratio of Pb(II) to sorption sites (Oyetade *et al.* 2016). Based on the intersection of the percentage removal and sorption capacity curves, 0.35 g of AC-PKS and 0.25 g AC-EDTA dosages were chosen for subsequent experiments, as they resulted in appreciable levels of Pb(II) percentage removal and sorption capacity.

Effect of initial Pb(II) concentration

The adsorption of Pb(II) on activated carbons as a function of the initial Pb(II) concentration is shown in Fig. 4. The results showed that the adsorption capacity (mg/g) increased with increasing Pb(II) concentration. AC-EDTA showed a higher adsorption of Pb(II) than AC-PKS. The Pb removal increased rapidly in both adsorbents for the first 20 min due to the high availability of the sorption sites but then gradually decreased and reached a plateau as the surface sites became saturated and the adsorption equilibrium was obtained. The time taken to reach equilibrium was longer for AC-EDTA, indicating more active sites were available on AC-EDTA.

With an increase in the initial concentration of Pb(II) solution from 50 to 150 mg/g, the extent of Pb(II) removal increased from 27 to 66.9 mg/g on AC-PKS and from 48 to 100.2 mg/g on AC-EDTA. This is because higher initial concentrations provide greater the driving force to overcome the resistance of Pb(II) ions between the aqueous and solid phase (Rafatullah *et al.* 2012). At low concentrations, the ratio of available surface to initial Pb(II) concentration was larger, so the removal became independent of initial concentrations, while in the case of higher concentrations, this ratio was low and the removal was dependent upon the initial concentration (Al-Othman *et al.* 2012).

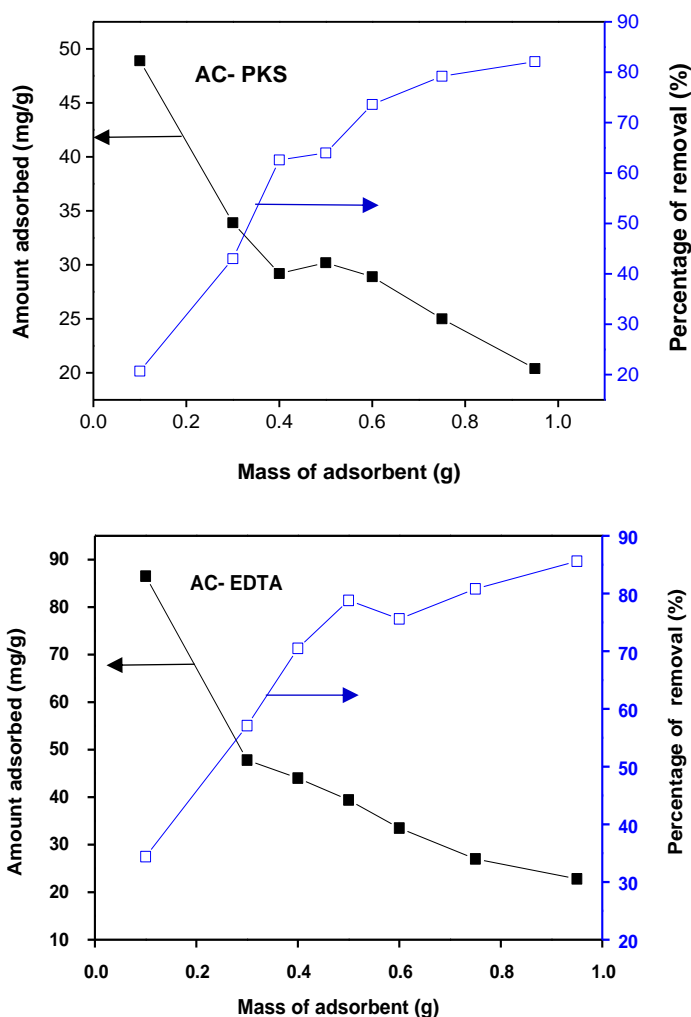


Fig. 3. Effect of (a) AC-PKS and (b) AC-EDTA dose on the sorption capacity and removal efficiency of Pb(II) from aqueous solution (Pb(II) concentration = 100 mg/L)

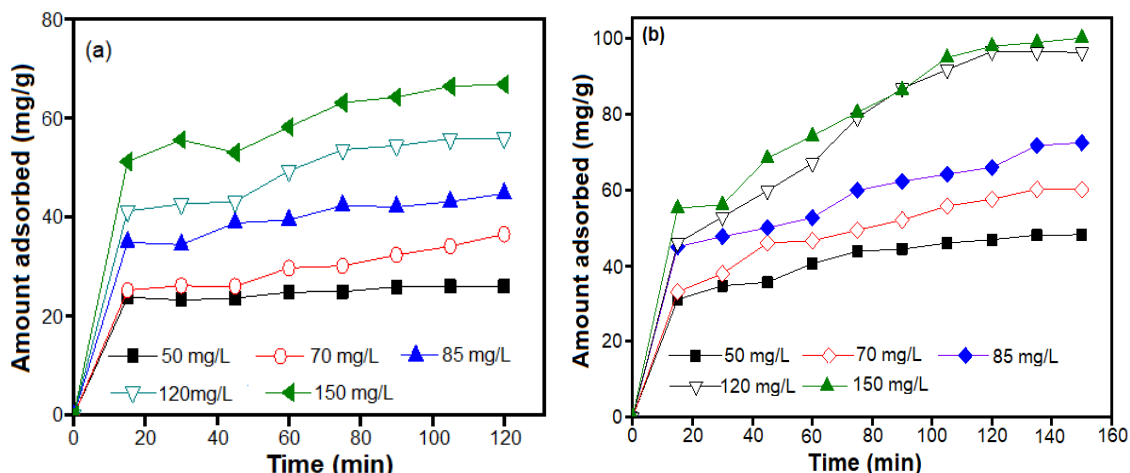


Fig. 4. Effect of time on adsorbed lead concentrations at different initial Pb(II) concentrations on (a) AC-PKS (0.35 g) (b) AC-EDTA (0.25 g)

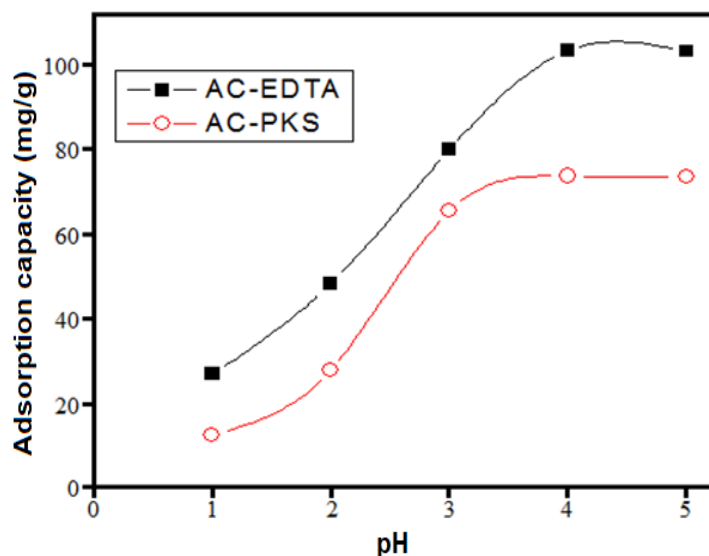


Fig. 5. Effects of initial solution pH on Pb adsorption onto AC-PKS and AC-EDTA (Adsorbent dosage = 0.35 g AC-PKS and 0.25 g AC-EDTA; Pb (II) concentration = 150 mg/L)

Effect of pH

The dependence of metal uptake on pH has direct connotation to both the metal chemistry in the solution and the ionization state of the functional groups, which affects the availability of binding sites (Farghali *et al.* 2013). The effect of pH on adsorption Pb(II) onto AC, as illustrated in Fig. 5, showed that the removal efficiency increased with the increase of pH up to 4 but did not change significantly when increased to pH 5. The Pb(II) uptakes were found to be low at pH < 4.0 because of the electrostatic repulsion between the cationic Pb(II) ions and the positively charged adsorbent surfaces. The abundant H⁺ ions could also be competing with Pb(II) ions for available binding sites. At pH 4, maximum amount of Pb(II) removed was 73.5 mg/g (68.6%) and 103.7 mg/g (69.1%) AC-PKS and AC-EDTA, respectively, which can be attributed to the electrostatic attraction between the negatively charged surface of the adsorbents and Pb(II) ions.

Overall, the adsorption of Pb(II) on AC-EDTA is higher than that of AC-PKS although it possess lower surface area. The enhancement in the Pb(II) adsorption was attributed to the presence of carboxyl group of EDTA that is capable of capturing the Pb(II) ions via surface complexation process.

Adsorption Isotherm, Kinetics, and Thermodynamics

Langmuir and Freundlich isotherms are the most common isotherm models used for describing adsorption characteristics of the adsorbents. These two adsorption isotherms were employed to investigate the interaction between the equilibrium concentration of Pb(II) and its uptake on AC-PKS and AC-EDTA. As shown in Table 2 the adsorption data fitted the Langmuir isotherm model, as the correlation coefficient for both activated carbons is close to unity, suggesting uniform and non-interacting sites of adsorption.

The comparative maximum adsorption capacity of Pb (II) ions on AC-EDTA with previously reported adsorbents is given in Table 3. The results revealed AC-PKS and AC-EDTA as promising adsorbents, with the adsorption capacity higher than other activated carbon produced from agriculture wastes for alleviation Pb (II) from aqueous solution. The superior performance of the AC-PKS shown in this work may be due to the use of phosphoric acid in the preparation of activated carbon. Phosphoric acid has been reported to produce activated carbon high degree of intrinsic pore structure with high percentage of micropores and mesopores (Rafatullah et al., 2012; Patnukao and Pavasant 2008). This could be responsible for the increase in homogenous adsorption sites with an ideal microstructure cross-section for enhanced Pb(II) uptake.

Table 2. Langmuir and Freundlich Isotherm Constants and Correlation Coefficients for Pb(II) Adsorption onto AC-PKS and AC-EDT

Adsorbents	Langmuir Isotherm			Freundlich Isotherm		
	Q_{\max} (mgg ⁻¹)	K_L	R^2	K_F	n	R^2
AC-PKS	80.6	1.209	0.9805	1.256	2.271	0.9559
AC-EDTA	104	0.260	0.9982	1.341	4.664	0.9673

Table 3. Comparison of Maximum Adsorption Capacities (Q_{\max}) of Pb(II) Ions by Activated Carbon Prepared from Different Sources

Adsorbent	Maximum Adsorption Capacity, Q_{\max} (mg/g)	References
Palm kernel shell (AC-PKS)	80.6	This study
AC-EDTA	104	This study
Coconut shell AC	26.5	Sekar <i>et al.</i> 2004
Coconut shell AC	26.1 - 49.9	Sharaf El-Deen & Sharaf El-Deen 2016
Tamarind wood AC	134.2	Singh <i>et al.</i> 2008
<i>Polygonum orientale</i> Linn AC	50 -75	Wang <i>et al.</i> 2010
Apricot stone AC	21.4	Mouni <i>et al.</i> 2011
Raffia Palm fruit Epicarp AC	28.0 - 66.4	Ghogomu <i>et al.</i> 2016

To determine the adsorption mechanism of Pb(II), the experimental data were subjected to different kinetic models, which included the pseudo-first-order, pseudo-second-order and intraparticle diffusion. The linearized form of the pseudo-first-order and pseudo-second order are represented in Eqs. 3 and 4, respectively,

$$\ln(q_e - q_t) = \ln q_e - k_1 t \quad (3)$$

$$\frac{t}{q_t} = \frac{1}{k_2 q_e^2} + \frac{1}{q_e} t \quad (4)$$

where k_1 and k_2 represents the rate constant for the pseudo-first and pseudo-second-order, while q_e and q_t are amount of metal ions adsorbed at equilibrium and at any given time t , respectively. As shown in Table 4, the coefficient of determination values (R^2) of the pseudo-second-order kinetic model were close to unity for both adsorbents, and the q_e experimental is close to the calculated q_e . Therefore, the pseudo-second order model appeared to be the best-fitting model for sorption process of Pb(II) on AC-PKS and AC-EDTA. This result suggested that the adsorption process is governed by the availability of the active adsorption sites rather than the concentration of Pb(II) in the bulk solution (Arshadi *et al.* 2014).

The diffusion mechanism for the sorption of Pb(II) onto AC-PKS and AC-EDTA was evaluated using the intraparticle diffusion model. The rate of intraparticle diffusion is a function of $t^{1/2}$ and the linearized form is represented in Eq. 5,

$$Q_t = K_d t^{1/2} + C \quad (5)$$

where K_d is the intraparticle diffusion rate constant ($\text{mg/g min}^{1/2}$) and C is the intercept.

Table 4. Pseudo-First Order and Pseudo-Second Order Constants for Pb(II) Adsorption

Adsorbent	Pseudo-first order				Pseudo-second order		
	q_e exp. (mg/g)	q_e calc. (mg/g)	k_1 (min^{-1})	R^2	Q_e calc. (mg/g)	k_2 ($\text{g mg}^{-1}\text{min}^{-1}$)	R^2
AC-PKS	56.0	70	0.014	0.9540	64.9	0.00101	0.9847
AC-EDTA	96.4	1.54	0.0268	0.9117	125	0.0002	0.9835

The plot for the intraparticle diffusion model for AC-PKS and AC-EDTA (Fig. 6(a-b)) showed multi-linearity with three different stages. The first stage corresponds to faster migration of Pb(II) towards AC-PKS and AC-EDTA surfaces *via* film diffusion. The second stage relates to the gradual uptake of Pb(II) through intraparticle diffusion, while the third stage defines the final equilibrium portion where the intraparticle diffusion began to slow down. The straight line did not pass through the origin of the plot, which confirmed that the film diffusion as well as intraparticle diffusion occurred concurrently during the Pb(II) sorption on AC-CA and AC-EDTA.

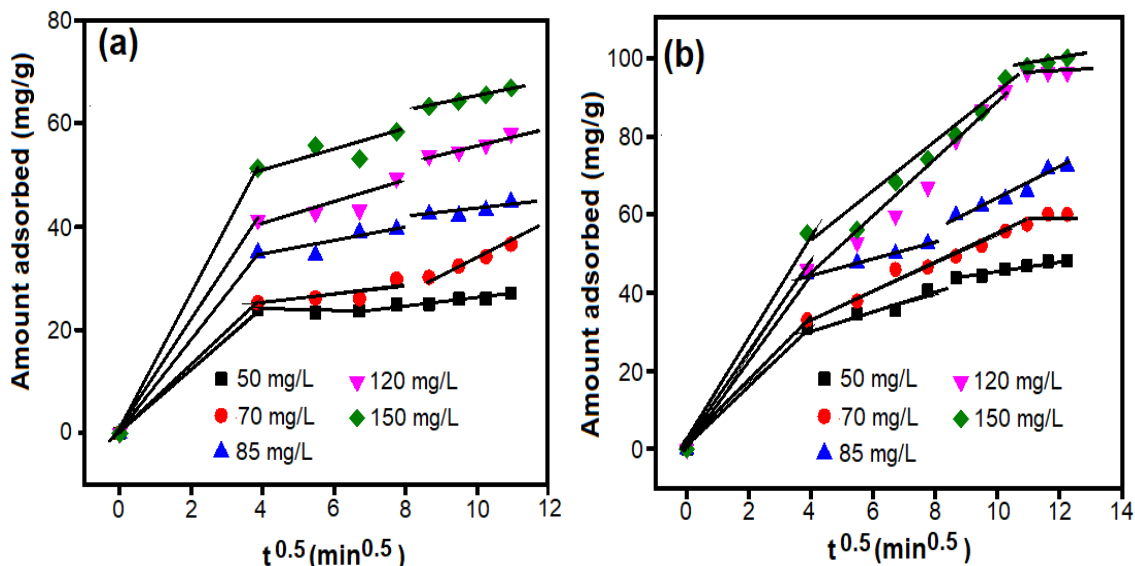


Fig. 6. The intraparticle kinetic modeling for Pb adsorption on to (a) AC-PKS and (b) AC-EDTA for different initial concentrations of Pb (Initial pH = 5; dosage = 0.35g AC-PKS and 0.25 g AC-EDTA)

Figure 7 shows the effect of temperature on adsorption of Pb onto AC-PKS and AC-EDTA. When the temperature was increased from 25 °C to 50 °C, the adsorption capacity increased from 80 to 91.5 mg/g (AC-CA) and 98.6 to 107.2 mg/g (AC-EDTA). However, the sorption capacity slightly decreased to 90.9 mg/g and 107.2 mg/g, respectively, over 50 °C. It is likely that the temperature was high enough to cause a higher rate of desorption than that of adsorption. To that effect, the determination of thermodynamic parameters was limited to an adsorption temperature of 50 °C.

The change in free energy (ΔG°), enthalpy ΔH° , and entropy ΔS° associated with the adsorption process were calculated with Eqs. 6, 7, and 8. ΔH° and ΔS° were calculated from Vant Hoff's equation (Eqs. 7 and 8),

$$\Delta G^\circ = -RT \ln K_C \quad (6)$$

$$\ln K_C = \left(\frac{\Delta S^\circ}{R}\right) - \left(\frac{\Delta H^\circ}{R}\right) \frac{1}{T} \quad (7)$$

$$K_C = C_{Ae}/C_{Se} \quad (8)$$

where K_C is the equilibrium constant, C_{Ae} is the amount of adsorbate on the adsorbent (mg/L), C_{Se} is the equilibrium concentration of adsorbate in the solution (mg/L), and R is the universal gas constant (8.314 J/ mol K). ΔH° and ΔS° were calculated from the slope and intercept of linear plot of $\ln K_C$ versus $1/T$.

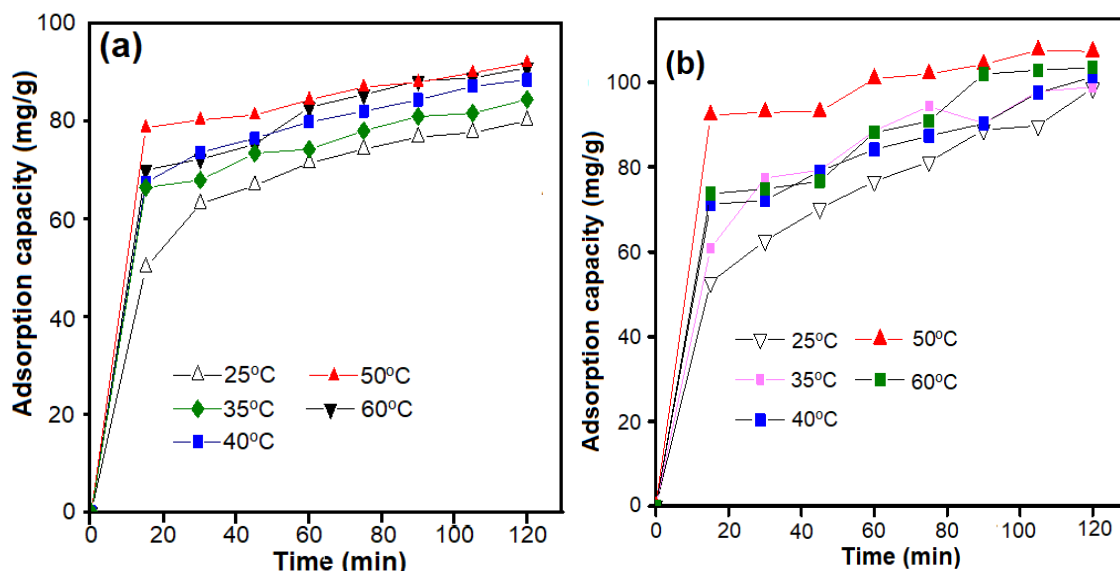


Fig. 7. Effect of temperature on Pb(II) adsorption on (a) AC-PKS (b) AC-EDTA (pH = 4; Dosage = 0.35 g AC-PKS and 0.25 g AC-EDTA and Pb (II) Co = 150 mg/L)

Table 5. Thermodynamic Parameters for the Adsorption of Pb(II) on AC-PKS and AC-EDTA at Various Temperatures

Temp (K)	AC-PKS					AC-EDTA				
	Q (mg/g)	lnK	ΔG° (kJ/mol)	ΔS° (J/Kmol)	ΔH° (kJ/mol)	Q (mg/g)	lnK	ΔG° (kJ/mol)	ΔS° (J/Kmol)	ΔH° (kJ/mol)
298	80	1.00	- 2.478	121.9	33.9	98.6	0.42	-1.041	82.5	23.6
308	84.4	1.28	- 3.278			98.8	0.66	-1.690		
313	88.4	1.75	- 4.55			101.2	0.73	-1.899		
323	91.5	2.02	- 4.307			107.2	1.20	-3.223		
333	90.9	1.85	- 5.010			103.4	0.80	-2.214		

The calculated ΔG° , ΔH° , and ΔS° are presented in Table 5. With increasing temperature, the ΔG° value became more negative, indicating the increase in the degree of spontaneity. This effect was attributed to the increase in the mobility and diffusion of the ions into the pore sites of the adsorbent. The positive value of ΔH° confirmed the endothermic nature of adsorption process.

Fixed-Bed Study

Analysis of breakthrough experimental data

The performance of a packed bed is described through the concept of the breakthrough curve, an important characteristic for determining and evaluating the sorbents for continuous treatment of the metal-laden effluents on an industrial scale operation. The breakthrough time (t_b) and the exhaustion time (t_e) shows the time at which the outlet Pb concentration reached 50% and exceeded 95% of the inlet Pb concentration (initial concentration), respectively.

The total amount of Pb(II) introduced into the column (M_{total}) and the total quantity of metal adsorbed in the column (Q_{total}) for a given feed concentration (C_o) and

flow rate (F) can be calculated from the following equations (Nethaji *et al.* 2013; Sukumar *et al.* 2017),

$$M_{total} = \frac{C_0 \times F \times t_e}{1000} \quad (9)$$

$$Q_{total} = \frac{F}{1000} \int_{t=0}^{t=t_{total}} (C_o - C_t) dt \quad (10)$$

where $(C_o - C_t)$ is the amount of adsorbed metal ion and F the flow rate (mL/min), calculated through dividing the effluent volume (V_{eff} , mL) by the total time (t_{total} , min). The total % removal can be calculated using Eq. 11.

$$\text{Total Pb(II) removal (\%)} = \frac{Q_{total}}{M_{total}} \times 100 \quad (11)$$

The equilibrium uptake capacity (Q_e , mg/g) of the AC-EDTA is determined by Eq. 12.

$$Q_e = \frac{Q_{total}}{M} \quad (12)$$

The mass transfer zone, where the adsorption happens, is calculated as follows,

$$MTZ = L \frac{t_e - t_b}{t_e} \quad (13)$$

where L is the adsorbent bed height (cm), t_b is the time required to reach the breakthrough point (min), and t_e is the time required for completion (min) of the adsorption.

The effect of the feed flow rate on the adsorption of Pb on AC-EDTA was depicted in Fig. 8(a). The breakthrough curves for the fast flow rate showed relatively early t_b and t_e , consequently resulting in less adsorption capacity. This may be due to the insufficient residence time for the Pb(II) ions within the bed and the limited diffusivity of the solute into the adsorptive sites or pores of the AC-EDTA (Muthusamy and Venkatachalam 2015). Longer residence time was observed in lower flow rates with high adsorption capacity.

Figure 8(b) shows the effect bed height had on the adsorption performance of AC-EDTA. The s-shape and the gradient of plotted breakthrough curves for the two heights vary slightly. The t_b and t_e values also increased as the bed depth increased, which led to higher adsorption capacity of Pb(II) on AC-EDTA (Table 6). This was attributed to longer mass transfer zone (Chowdhury *et al.* 2013), and the availability of more adsorption sites thereby resulting in an extended breakthrough time.

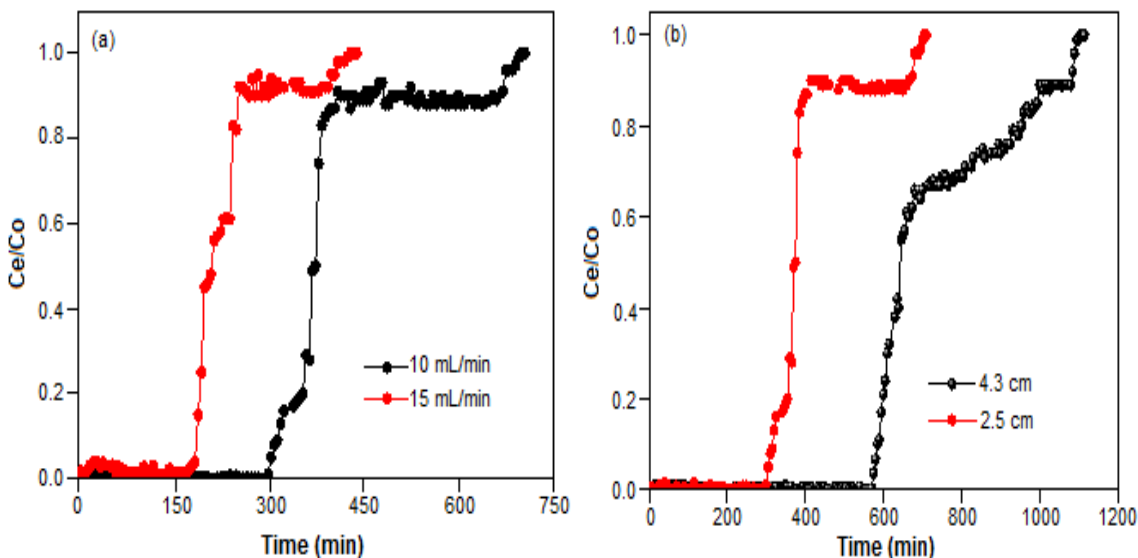


Fig. 8. Breakthrough curves for adsorption by Pb(II) onto AC-EDTA at (a) different flow rates (Pb(II) = 150 mg/L; Bed height = 2.5 cm) and (b) bed height (flow rate = 10 mL/min)

Table 6. Breakthrough Parameters for Pb(II) Adsorption on to AC-EDTA

Column Condition				Breakthrough Analysis			
C_o (mg/L)	Bed height (cm)	Flow rate (mL/min)	t_b (min)	Uptake Q (mg/g)	Pb(II) removal (%)	t_e (min)	MTZ (cm)
150	4.3	10	600	154.8	93.4	1105	2.59
150	2.5	10	400	98.8	93.4	750	1.68
150	2.5	15	199	90.4	93.3	430	1.78

CONCLUSIONS

1. Activated carbon prepared from palm kernel shells was successfully modified with EDTA.
2. The surface modification of AC-PKS resulted in a decrease in surface area and porosity of the activated carbon.
3. Adsorption of Pb(II) on AC-PKS and AC-EDTA followed Langmuir adsorption isotherm models pseudo-second order kinetic model.
4. The AC-EDTA showed higher adsorption capacity than the AC-PKS.
5. The optimum conditions for batch adsorption were 0.25 g AC-EDTA, 150 mg/L of Pb(II) solution, and pH 4.

ACKNOWLEDGMENTS

The first author gratefully acknowledges Federal University Lokoja, Nigeria, for the study leave granted to carry out this research and TETFUND for the financial support.

REFERENCES CITED

- Al-Othman, Z. A., Ali, R., and Naushad, M. (2012). "Hexavalent chromium removal from aqueous medium by activated carbon prepared from peanut shell: Adsorption kinetics, equilibrium and thermodynamic studies," *Chem. Eng. J.* 184, 238-247. DOI: 10.1016/j.cej.2012.01.048
- Arshadi, M., Amiri, M. J., and Mousavi, S. (2014). "Kinetic, equilibrium and thermodynamic investigations of Ni(II), Cd(II), Cu(II) and Co(II) adsorption on barley straw ash," *Water Resour. Ind.* 6, 1-17. DOI: 10.1016/j.wri.2014.06.001
- Biswas, S., and Mishra, U. (2015). "Continuous fixed-bed column study and adsorption modeling: Removal of lead ion from aqueous solution by charcoal originated from chemical carbonization of rubber wood sawdust," *Journal of Chemistry* 2015, Article ID 907379. DOI: 10.1155/2015/907379
- Chowdhury, Z. Z., Hamid, S. B. A., Das, R., Hasan, M. R., Zain, S. M., Khalid, K., and Uddin, M. N. (2013). "Preparation of carbonaceous adsorbents from lignocellulosic biomass and their use in removal of contaminants from aqueous solution," *BioResources* 8(4), 6523-6555. DOI: 10.15376/biores.8.4.6523-6555
- Ding, Y., Liu, Y., Liu, S., Li, Z., Tan, X., Huang, X., Zeng, G., Zhou, Y., Zheng, B., and Cai, X. (2016). "Competitive removal of Cd(II) and Pb(II) by biochars produced from water hyacinths: performance and mechanism," *RSC Adv.* 6(7), 5223-5232. DOI: 10.1039/C5RA26248H
- Farghali, A. A., Bahgat, M., Enaiet Allah, A., and Khedr, M. H. (2013). "Adsorption of Pb(II) ions from aqueous solutions using copper oxide nanostructures," *Beni-Suef Univ. J. Basic Appl. Sci.* 2, 61-71. DOI: 10.1016/j.bjbas.2013.01.001
- Jumasiah, A., Chuah, T. G., Gimbon, J., Choong, T. S. Y., and Azni, I. (2005). "Adsorption of basic dye onto palm kernel shell activated carbon: Sorption equilibrium and kinetics studies," *Desalination* 186(1-3), 57-64. DOI: 10.1016/j.desal.2005.05.015
- Kampalananwat, P., and Supaphol, P. (2014). "The study of competitive adsorption of heavy metal ions from aqueous solution by aminated polyacrylonitrile nanofiber mats," *Energy Procedia* 56, 142-151. DOI: 10.1016/j.egypro.2014.07.142
- Mohammadnezhad, G., Soltani, R., Abad, S., and Dinari, M. (2017). "A novel porous nanocomposite of aminated silica MCM-41 and nylon-6: Isotherm, kinetic, and thermodynamic studies on adsorption of Cu(II) and Cd(II)," *Journal of Applied Polymer Science* 134(40), 45383. DOI: 10.1002/app.45383
- Mouni, L., Merabet, D., Bouzaza, A., and Belkhir, L. (2011). "Adsorption of Pb(II) from aqueous solutions using activated carbon developed from apricot stone," *Desalination* 276(1), 148-153. DOI: 10.1016/j.desal.2011.03.038
- Muthusamy, S., and Venkatachalam, S. (2015). "Advances single- and binary-metal systems onto a biodiesel," *RSC Adv.* 5(45), 45817-45826. DOI: 10.1039/C5RA05962C
- Nowicki, P., Kuszyńska, I., Przepiórski, J., and Pietrzak, R. (2013). "The effect of chemical activation method on properties of activated carbons obtained from pine cones," *Cent. Eur. J. Chem.* 11(1), 78-85. DOI: 10.2478/s11532-012-0140-0
- Oyetade, O. A., Nyamori, V. O., Martincigh, B. S., and Jonnalagadda, S. B. (2016). "Nitrogen-functionalised carbon nanotubes as a novel adsorbent for the removal of Cu(II) from aqueous solution," *RSC Adv.* 6(4), 2731-2745. DOI: 10.1039/c5ra23900a
- Patnukao, P., and Pavasant, P. (2008). "Activated carbon from Eucalyptus camaldulensis

- Dehn bark using phosphoric acid activation," *Bioresource Technology* 99, 8540-8543. DOI: 10.1016/j.biortech.2006.10.049
- Rafatullah, M., Sulaiman, O., Hashim, R., and Ahmad, A. (2012). "Removal of cadmium (II) from aqueous solutions by adsorption using meranti wood," *Wood Sci. Technol.* 46 (1-3), 221-241. DOI: 10.1007/s00226-010-0374-y
- Reddy, N. A., Lakshmiopathy, R., and Sarada, N. C. (2014). "Application of *Citrullus lanatus* rind as biosorbent for removal of trivalent chromium from aqueous solution". *Alexandria Eng. J.* 53(2), 969-975. DOI: 10.1016/j.aej.2014.07.006
- Sekar, M., Sakthi, V., and Rengaraj, S. (2004). "Kinetics and equilibrium adsorption study of lead(II) onto activated carbon prepared from coconut shell," *J. Colloid Interface Sci.* 279(2), 307-313. DOI: 10.1016/j.jcis.2004.06.042
- Sharaf El-Deen, G. E., and Sharaf El-Deen, S. E. A. (2016). "Kinetic and isotherm studies for adsorption of Pb(II) from aqueous solution onto coconut shell activated carbon," *Desalin. Water Treat.* 57(59), 28910-28931. DOI: 10.1080/19443994.2016.1193825
- Singh, C. K., Sahu, J. N., Mahalik, K. K., Mohanty, C. R., Mohan, B. R., and Meikap, B. C. (2008). "Studies on the removal of Pb(II) from wastewater by activated carbon developed from Tamarind wood activated with sulphuric acid," *J. Hazard. Mater.* 153(1), 221-228. DOI: 10.1016/j.jhazmat.2007.08.043
- Sukumar, C., Janaki, V., Vijayaraghavan, K., Kamala-Kannan S., and Shanthi, K. (2017). "Removal of Cr(VI) using co-immobilized activated carbon and *Bacillus subtilis*: Fixed-bed column study," *Clean Technol. Environ. Policy* 19(1), 251-258 DOI: 10.1007/s10098-016-1203-2
- Sulaymon, A. H., Mohammed, A. A., and Al-Musawi, T. J. (2013). "Competitive biosorption of lead, cadmium, copper, and arsenic ions using algae," *Environ. Sci. Pollut. Res.* 20(5), 3011-3023. DOI: 10.1007/s11356-012-1208-2
- Thommes, M., Kaneko, K., Neimark, A. V., Olivier, J. P., Rodriguez-reinoso, F., Rouquerol, J., and Sing, K. S. W. (2015). "Physisorption of gases, with special reference to the evaluation of surface area and pore size distribution (IUPAC Technical Report)," *Pure Appl. Chem.* 87(9-10), 1051-1069. DOI: 10.1515/pac-2014-1117
- Tofan, L., Paduraru, C., Volf, I., and Toma, O. (2011). "Waste of rapeseed from biodiesel production as a potential biosorbent for heavy metal ions," *BioResources* 6(4), 3727-3741. DOI: 10.15376/biores.6.4.3727-3741
- Tongpoothorn, W., Sriuttha, M., Homchan, P., Chanthai, S., and Ruangviriyachai, C. (2011). "Preparation of activated carbon derived from *Jatropha curcas* fruit shell by simple thermo-chemical activation and characterization of their physico-chemical properties," *Chem. Eng. Res. Des.* 89, 335-340. DOI: 10.1016/j.cherd.2010.06.012
- Wang, L., Zhang, J., Zhao, R., Li, Y., Li, C., and Zhang, C. (2010). "Adsorption of Pb (II) on activated carbon prepared from *Polygonum orientale* Linn: Kinetics, isotherms, pH, and ionic strength studies," *Bioresource Technol.* 101(15), 5808-5814. DOI: 10.1016/j.biortech.2010.02.099
- Wang, L., and Li, J. (2013). "Removal of methylene blue from aqueous solution by adsorption onto crofton weed stalk," *BioResources* 8(2), 2521-2536. DOI: 10.15376/biores.8.2.2521-2536

Wang, Z., Shirley, M. D., Meikle, S. T., Whitby, R. L. D., and Mikhalovsky, S. V. (2008). "The surface acidity of acid oxidised multi-walled carbon nanotubes and the influence of in-situ generated fulvic acids on their stability in aqueous dispersions," *Carbon* 47(1), 73-79. DOI: 10.1016/j.carbon.2008.09.038

Article submitted: September 9, 2017; Peer review completed: November 18, 2017;
Revised version received: December 14, 2017; Accepted: December 15, 2017; Published:
January 5, 2018.
DOI: 10.15376/biores.13.1.1235-1250